SIMPLE MODELS FOR BEAM LOSS NEAR THE HALF INTEGER RESONANCE WITH SPACE CHARGE

C. M. Warsop, D. J. Adams, B. Jones, B. G. Pine, ISIS, Rutherford Appleton Laboratory, U.K.

Abstract

The half integer resonance is often used to define the high intensity limit of medium or low energy hadron rings where transverse space charge is significant. However, the mechanism leading to particle loss as beam approaches this resonance, which thus defines the limit, is not clearly understood. In this paper we explore simple models, based on single particle resonance ideas, to see if they describe useful aspects of motion as observed in simulations and experiments of 2D coasting beams on the ISIS synchrotron. Single particle behaviour is compared to 2D self-consistent models to assess when coherent motion begins to affect the single particle motion, and understand the relevance of coherent and incoherent resonance. Whilst the general problem of 2D resonant loss, with non-stationary distributions and non-linear fields is potentially extremely complicated, here we suggest that for a well-designed machine (where higher order pathological loss effects are avoided) a relatively simple model may give valuable insights into beam behaviour and control.

INTRODUCTION

Background

The half integer resonance is often taken as defining the high intensity limit of hadron rings, where there is the expectation that lower order, quadrupole errors will drive the dominant loss. However, the details of mechanisms driving particle emittance growth and loss as beam approaches resonance are not well understood.

Whilst the well known intensity limit based on the incoherent tune shift gives a useful rule of thumb, it over estimates losses as it neglects coherent motion of the beam [1]. The coherent model, on the other hand, gives a fuller, self-consistent picture by taking into account the envelope modulation, and predicts resonance at the higher, coherent limit. However, coherent theory is based on Kapchinskij-Vladimirskij (KV) distributions and RMS equivalent models that are only valid as long as RMS emittances are conserved, i.e. when there is no emittance growth. Therefore, they cannot be used to understand particle motion and loss as beam approaches resonance. To derive models to explain such losses, a modified single particle model is required that includes the effect of the coherent response of the beam.

As a first step, this paper analyses single particle motion in the frozen space charge case for a representative waterbag beam. An initial comparison with coherent theory is also given. Future work will build on these results, exploring their limitations with detailed self-consistent simulations.

Building on Experimental Results from ISIS

The idea that single particle models should be useful for describing half integer resonance comes from experimental observations on the ISIS proton synchrotron [2]. Extensive experimental and simulation work studying the approach of half integer resonance in 2D coasting beams have characterized the evolution of transverse beam profiles in detail [2, 3]. Comparison of these results with comprehensive ORBIT models indicated that "lobe" features on profiles corresponded to half integer resonant islands. This suggests that a useful starting point for models is single particle theory, with the expectation that corrections for coherent effects will be required.

Below we calculate particle trajectories for resonant particle motion in a frozen space charge model, next we analyse the main dependencies this predicts for driving term strength, tune and intensity. Finally, we discuss and compare predictions with those from coherent theory, and outline future work.

FROZEN WATERBAG MODEL

This analysis considers the motion of a test particle, in a smooth focusing system, in the space charge field of a *frozen* waterbag beam distribution. This distribution is chosen as a representative case that includes key features a KV distribution does not: it has tune variation with amplitude and is non-stationary. It is the initial motion of this non-stationary distribution that we are interested in for studying the onset of resonance. This non-stationary waterbag beam would redistribute in any realistic *non-frozen* beam model, and this means the Hamiltonian derived below is certainly not an invariant over long time scales. Usually the type of analysis used here assumes resonance with long term invariance with KV beams, e.g. [4]. However, what is of interest here is the short term motion of a beam; its initial redistribution as it approaches resonance. Therefore, we use this *"short term invariant"* to predict the initial trajectories of particles, before the beam redistributes significantly. This should indicate how the beam behaves on approaching resonance.

The analysis of particle motion is made difficult by the piecewise definition required for the space charge potential inside and outside the waterbag beam. This complication is removed using the method of phase averaging, following work in [4]. This gives a smoothed action-angle approximation, from which we can extract particle motion.

Phase Averaged Hamiltonian

We analyse the motion of a test particle in the field of a 4D, axisymmetric waterbag beam with radius a of the form $n(r) = n_0(1 - \frac{r^2}{a^2})$, (for $r \le a$, zero otherwise) with $r^2 =$

$x^2 + y^2$. We consider motion of particles in one plane only, e.g. the $y = 0$ plane, so $r = x$. The motion of the beam in one dimension is defined in canonical coordinates (x, P_x), with periodic "time" dependence s, via the quadrupole driving term $K_d(s)$, in a smooth focusing system with zero intensity tune $\omega = \frac{Q}{R}$. The periodic system corresponds to a ring of mean radius R with betatron tune Q. The Hamiltonian is:

$$H(x, P_x, s) = \tfrac{1}{2}P_x^2 + \tfrac{1}{2}\omega^2 x^2 + K_d(s)x^2 + V(x), \quad (1)$$

where the space charge potential $V(x)$ is defined in a piece-wise way as:

$$V(x) = \begin{cases} V_i = -k(\frac{x^2}{a^2} - \frac{x^4}{4a^4}), & \text{if } x \le a, \\ V_o = -k(\frac{3}{4} + \log\frac{|x|}{a}), & \text{if } x > a, \end{cases} \quad (2)$$

with $k = \frac{q^2 N}{2\pi\epsilon_0 mc^2\beta^2\gamma^3}$ the perveance, q and m the particle charge and mass, N the number line density, c the speed of light and β and γ relativistic parameters.

To perform the phase averaging we now transform to action-angle variables (ϕ, J) defined by:

$$x = \sqrt{\frac{2J}{\omega}}\sin\phi; \quad P_x = \sqrt{2J\omega}\cos\phi, \quad (3)$$

and then the aim is to determine $\overline{H} = \overline{H(\phi, J, s)} = \frac{1}{2\pi}\int_0^{2\pi} H(\phi, J, s)d\phi$, the Hamiltonian averaged over one betatron oscillation. The system is assumed to be near resonance. Equation (3) is substituted into (1) and (2), and the integrations completed.

It is convenient to split the Hamiltonian (1) into two parts, the simpler first three terms H_0 and the piecewise final term, that we average to find $\overline{V(J)}$. Phase averaging over H_0, with the assumption that the system is near a single half integer resonance, $2Q = l\theta$, with $\theta \equiv \theta(s) = \frac{s}{R}$, leads to the usual, well known result. The driving term is periodic with one dominant term: $K_d(s) = k_l \cos l\theta$, and we find

$$H_0 = \omega J + \frac{k_l J}{2\omega}\cos(2\phi - l\theta). \quad (4)$$

The full Hamiltonian is now $\overline{H} = H_0 + \overline{V(J)}$, where the last term is the result of phase averaging over the piecewise potential (2). This, when expanded in action-angle coordinates, becomes

$$V_i = -\frac{k}{a^2}\left[\frac{J}{\omega}\left(1 - \cos 2\phi\right) \right. $$
$$\left. - \frac{J^2}{\omega^2 a^2}\left(\frac{3}{8} - \frac{1}{2}\cos 2\phi + \frac{1}{8}\cos 4\phi\right)\right], \quad (5)$$

$$V_o = -k\left[\log\left(\sqrt{\frac{2J}{\omega a^2}}|\sin\phi|\right) + \tfrac{3}{4}\right]. \quad (6)$$

The phase averaging calculation depends on whether the test particle has an amplitude such that it is always within the beam (*core*), or one that exceeds the beam radius for some of the oscillation (*halo*). It is useful to define the normalised amplitude (as in [4]) given by $\sigma = x/a = \sqrt{2J/\omega a^2}$, where

$\sigma = 1$ or $J = J_a = \omega a^2/2$, corresponds to the beam edge. For a particle always within the beam $J \le J_a$, $\sigma \le 1$ the phase averaging is just over the V_i term in (5).

$$\overline{V_c} = I_0 = \frac{1}{2\pi}\int_0^{2\pi} V_i\,d\phi. \quad (7)$$

This gives a simple result, as oscillating terms average to zero (in the absence of driving terms, and in the incoherent approximation):

$$I_0 = k\left[-\frac{1}{a^2\omega}J + \frac{3}{8}\frac{1}{a^4\omega^2}J^2\right]. \quad (8)$$

For a particle of an amplitude $J > J_a$, $\sigma > 1$, it is useful to define the angle ϕ_1 with $\sin\phi_1 = 1/\sigma$. This defines the phase at which the test particle crosses the beam boundary. To achieve the averaging we integrate over a representative part of the oscillation: the internal potential V_i is integrated from $\phi = 0 \rightarrow \phi_1$ and the external V_o from $\phi = \phi_1 \rightarrow \pi/2$:

$$\overline{V_h} = I_1 + I_2 = \frac{2}{\pi}\left[\int_0^{\phi_1} V_i\,d\phi + \int_{\phi_1}^{\frac{\pi}{2}} V_o\,d\phi\right]. \quad (9)$$

The results of these integrations are

$$I_1 = -\frac{k}{a^2}\left[\frac{J}{\omega}\left(\phi_1 - \frac{1}{2}\sin 2\phi_1\right) \right.$$
$$\left. - \frac{J^2}{w^2 a^2}\left(\frac{3}{8}\phi_1 - \frac{1}{4}\sin 2\phi_1 + \frac{1}{32}\sin 4\phi_1\right)\right], \quad (10)$$

and

$$I_2 = -k\left[\frac{3}{4}\left(\frac{\pi}{2} - \phi_1\right) + F(\sigma)\right]. \quad (11)$$

where the integral $F(\sigma) = \int_{\phi_1}^{\pi/2} \log(\sigma|\sin\phi|)d\phi$, $(\phi_1 > 0)$ is not defined in terms of normal functions, but in the domain relevant here is simple in form and easily tabulated, see Fig. 1.
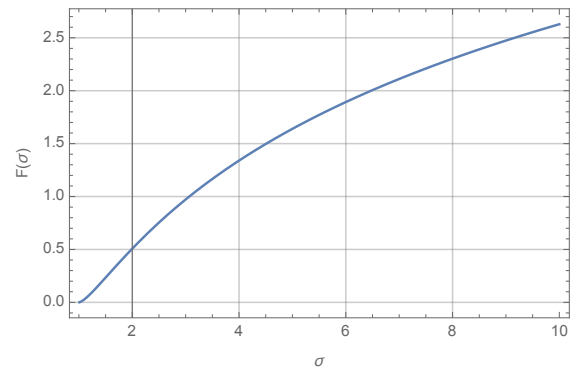

Figure 1: The function $F(\sigma)$.

The s dependence due to resonance in H_0 (4) is removed via a canonical transformation with an F_2 generating function and associated equations:

$$F_2 = \bar{J}(\phi - \frac{l}{2}\frac{s}{R}); \quad (12)$$
$$J = \bar{J}; \quad \bar{\phi} = \phi - \frac{l}{2}\frac{s}{R}; \quad \bar{H} = H - \frac{l}{2R}J.$$

The result is

$$\overline{H} = \overline{H(J,\bar\phi)} = \delta J + S J \cos 2\bar\phi + \overline{V(J)}, \qquad (13)$$

where $\delta = (\omega - \frac{l}{2R}) = \frac{1}{R}(Q - \frac{l}{2})$, $S = \frac{k_l}{2\omega}$ and,

$$\overline{V(J)} = \begin{cases} V_c = I_0 & \text{if } J \le J_a \quad (core). \\ V_h = I_1 + I_2 & \text{if } J > J_a \quad (halo). \end{cases} \qquad (14)$$

Essentials of Particle Motion

We now look at the predictions of this model, using the example of a nominal coasting beam in the ISIS ring. Resonance in just one plane is considered, $2Q_y = 7$ (particles are assumed to have zero amplitude in the orthogonal plane). The relevant parameters are: $Q_y = 3.60$, $R = 26$ m, $a = 0.05$ m, $l = 7$, $\Delta k_7 = 0.005$ ($\Delta k_7 = k_7/k = 2k_7/\omega^2$), and $N_p = 4.4 \times 10^{13}$ ppp (protons per pulse, where $N = N_p/(2\pi R)$). By setting the driving strength $\Delta k_7 = 0$ and using numerical solutions for $F(\sigma)$ and its derivative we can calculate the frequency variation with J, i.e. $w(J) = Q(J)/R = \frac{\partial H(J)}{\partial J}$. This is shown in Fig. 2.
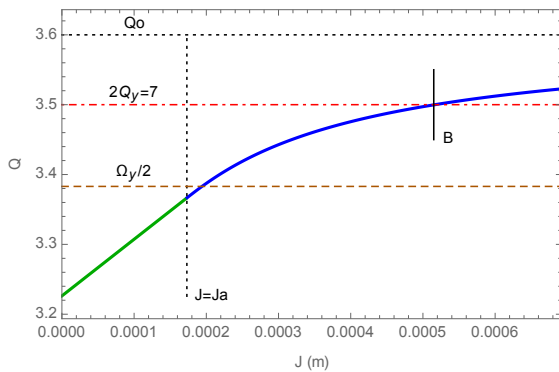

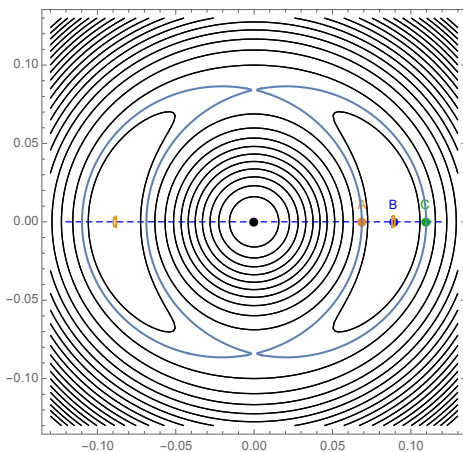Figure 2: Example of $Q(J)$ for waterbag beam (see text).

Figure 3: Example of $\overline{H}$ for waterbag beam, normalized coordinates $(x, P_x/\omega)$ in metres (see text).

The system is a non-linear oscillator with a frequency characterized by the $Q(J)$ dependence above. Single particle resonance, i.e. the stable fixed point, coincides with

the intercept of the $Q(J)$ curve with the $Q_y = 3.5$ line in Fig. 2 (point "B"). Contours of the *"short term invariant"* surface $\overline{H}$, equation (13) are shown in Fig. 3. The contours of this surface give an indication of the initial trajectories of particles, of the nominally matched beam, here of radius 0.05 m. Of particular interest is the stable fixed point ("B" in Fig. 3), and also the inner and outer limits of the separatrix and their intercepts with the x-axis (points "A" and "C" in Fig. 3). The fixed points are calculated in the normal way, using $\dot\phi = 0$, $\dot J = 0$ with Hamilton's equations, and the separatrix being the contour that passes through the unstable fixed point. Particles drawn along trajectories corresponding to the contours shown will either be confined in the central core region, drawn outward to oscillate about the the fixed points at the centre of the two resonant islands, or else make larger oscillations around both islands. The two resonant islands are expected to correspond to "lobes" observed in transverse profile measurements on ISIS. This model now allows us to predict the variation of the location and extent of these lobes with respect to beam parameters.

Comparison with Simple Tracking Results

The results presented here, $Q(J)$ and $\overline{H}$, have been compared with tunes and Poincaré maps from simple 1D particle tracking results, where motion was integrated directly and piecewise potentials explicitly included. Results show good agreement within the expected approximations.
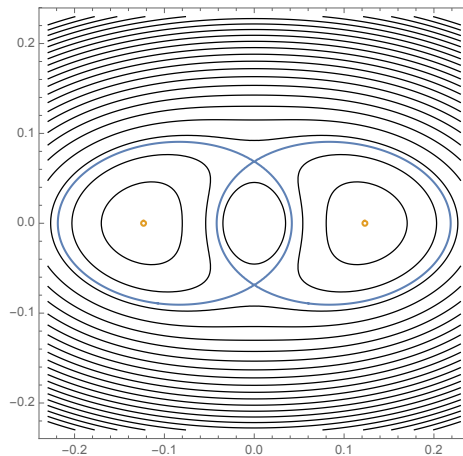

Figure 4: $\overline{H}$ with increased driving term strength Δk_7, note change in scale (see text).

PREDICTIONS OF MODEL

Continuing with the simplified example of ISIS, the dependence of $Q(J)$, $\overline{H}$ on beam parameters is now investigated.

Effect of Driving Term Strength

Beam parameters assumed are $Q_y = 3.60$, $R = 26$ m, $a = 0.05$ m, $l = 7$, $N_p = 4.4 \times 10^{13}$ ppp and various values of Δk_7. Results for $\Delta k_7 = 0.005$ are shown in Fig. 3. When $k_7 = 0$ the lobes disappear and contours become circular. Setting $\Delta k_7 = 0.05$ gives the result in Fig. 4. The

results show that the effect of increasing driving strength is to increase asymmetry and enlarge the extent of the two resonant lobes, whilst reducing the size of the central core region. In Fig. 5 we show in detail the variation of the stable fixed point and inner and outer limits of the separatrices (points "A", "B" and "C" defined in Fig. 3) with driving strength.
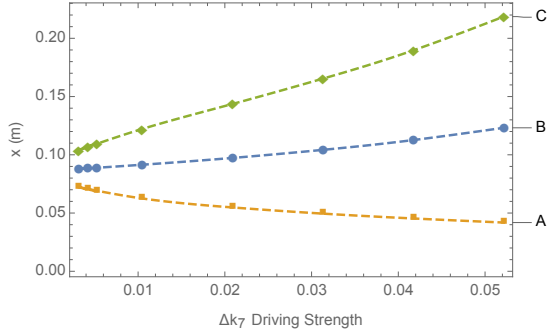

Figure 5: Dependence of island location and size on driving term strength.
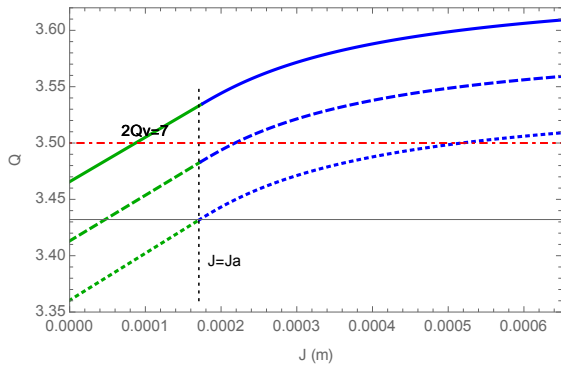

Figure 6: $Q(J)$ as a function of lattice Q (see text).

Figure 7: $\overline{H}$ with raised $Q = 3.65$ (see text).

Effect of Q

The effect of varying lattice tune $Q = \omega/R$ is now examined. Beam parameters are $R = 26$ m, $a = 0.05$ m, $l = 7$,

$N_p = 2.2 \times 10^{13}$ ppp. In Fig. 6, the dependence $Q(J)$ is shown for $Q = 3.65,\ 3.60,\ 3.55$ (top to bottom), $\Delta k_7 = 0$. The results show that as the lattice tune moves down, so the $Q(J)$ intercept with $Q_y = 3.5$, the stable fixed point and islands, move outward through the beam. In Fig. 7 the surface of $\overline{H}$ is shown for $Q = 3.65,\ \Delta k_7 = 0.005$: the stable fixed points are near the core of the beam as expected. This suggests that higher Q values may perturb the core a little, but generate smaller halo than lower tunes, where location of the stable fixed point suggests particles (and profile lobes) would be pulled further out from the core.

Effect of Intensity

The dependence of $Q(J)$ for three different intensities $N_p = 1.1,\ 2.2,\ 4.4 \times 10^{13}$ ppp, (top to bottom), is shown in Fig. 8, with parameters: $Q = 3.60,\ R = 26$ m, $a = 0.05$ m, $l = 7$, and $\Delta k_7 = 0$. In this case the effect is to move the stable fixed point from the core to the outside of the beam as intensity increases, with a corresponding movement of the resonant islands and profile lobes.
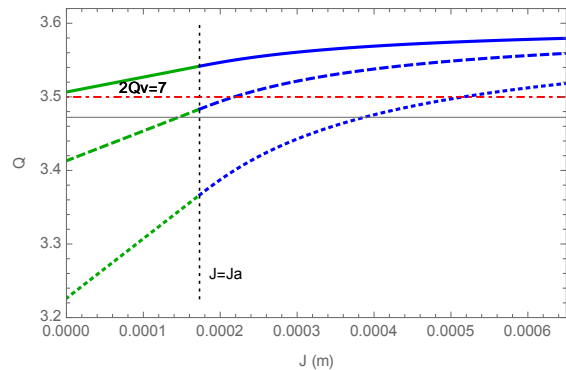

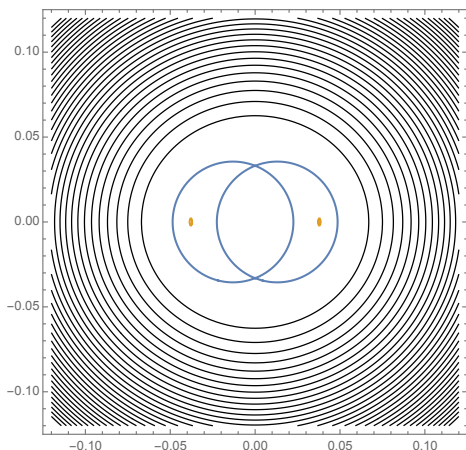Figure 8: $Q(J)$ as a function of intensity (see text).

Effect of Dynamic Intensity and Q Ramps

In a situation with a real beam, often the parameters above will change with time. For example, during multi-turn injection, intensity will ramp over 100s of turns. One might expect the situation in Fig. 8 to be descriptive, with the tunes in the beam pushing down with intensity and the separatrices moving correspondingly outward. Similarly, ramping the tune by changing quadrupoles in the lattice may give a dynamic situation related to Fig. 6. This simple picture ignores many complications, as discussed below.

LIMITATIONS OF THE MODEL

Non-Stationary Distribution, Mismatch

The fact that the waterbag distribution is non-stationary means that over long time scales the above analysis will not predict particle trajectories. If, in addition, beams are strongly mismatched, then redistribution may be faster and correspondence to the above analysis weaker. However, it may be that once the beam has redistributed and "grown",

the above model, with a modified beam radius, will give a first estimate of behaviour.

Coherent Motion

As noted, the above model is not self-consistent, and thus *ignores any coherent response* of the beam. Coherent effects will, in general, modify space charge fields and particle motion. Near coherent resonance effects on the beam are expected to be strong and a frozen single particle model to have limited value. However, further away from resonance effects will be weaker, and single particle models would be expected to explain main features of the motion, perhaps with some smaller modifications.

The dependence of coherent frequency of the beam envelope on space charge can be estimated using the concept of equivalent beams [1]. We expect the RMS parameters and resonant frequencies of our waterbag beam to behave in the same way as a KV beam with the same RMS emittance (ϵ_{RMS}). The edge of the 4D waterbag beam is at $6\epsilon_{\mathrm{RMS}}$. Assuming a circular beam and the large tune split approximation valid for ISIS (nominal tunes $(Q_x, Q_y) = (4.31, 3.83)$), we find coherent frequencies using (in the notation of [1]):

$$\Omega_y = \sqrt{4Q_y^2 - 5Q_x\Delta Q_x} \qquad (15)$$

with $\Delta Q_x = r_p N_p/(2\pi\beta^2\gamma^3 4\epsilon_{\mathrm{RMS}})$, r_p is the proton radius. This theory is two dimensional and provides coherent frequencies in both planes, but for this 1D model only one plane is relevant.

An example is shown in Fig. 2, where $\frac{\Omega_y}{2}$ is shown as the horizontal dashed line. This is expected to sit above the peak incoherent shift (as the coherent intensity limit is higher than the incoherent) [1], and its relative position will scale proportionately with intensity. When the driving frequency ($2Q_y = 7$ line) approaches the coherent frequency $\frac{\Omega_y}{2}$, then coherent resonance is expected with large coherent envelope oscillations and associated beam redistribution. Otherwise, coherent effects will be less pronounced and predictions of the single particle model will be more useful (with modification).

In Fig. 2, the system is away from coherent resonance: lowering the intensity would move the coherent tune upward towards resonance. This gives a first indication of when coherent effects will dominate: future work will make more use of predictions of RMS envelope motion to modify the above model, and test the results in detail with simulations.

2D Motion, Higher Order Effects

The work above ignores the motion of particles with finite emittance in the plane orthogonal to resonance. Assuming no additional resonance or coupling, one may expect the average effect to be a reduced average tune shift for larger amplitude particles, as they spend less time in the core of the beam. Future work will investigate this in more detail. The possibility of other resonances and space charge (particularly octupole) terms also need to be considered.

SIMULATIONS AND EXPERIMENTS

Comparison with Simulations

Work is presently underway comparing the results above with output from 2D self-consistent simulations (using the ISIS SET code). Initial results show reasonable agreement of incoherent frequency distributions and coherent frequencies between the above model and a simulated waterbag beam. There is also some correspondence between phase space distributions and phase space structure predicted above, but more detailed analysis is required.

Comparison with Experiments

ISIS experiments, where coasting high intensity beams are pushed onto the half integer resonance are described in [2, 3]. In these experiments profiles were observed to form a lobe on each side of the central beam distribution, corresponding to the resonant islands discussed above. The size and distance of these with respect to the central beam core has been measured as a function of driving strength and tune. The lobes were observed to move outward with increasing driving term strength and also outward as the tune was lowered. This is in *qualitative* agreement with the predictions above. However, more work is required to address the approximations in the model and thus allow a more useful *quantitative* comparison.

SUMMARY

The *"short term invariant"* Hamiltonian for a frozen waterbag beam has been calculated using the method of phase averaging. This has been used to give predictions of the dependence of halo structure on parameters of driving strength, tune and intensity. The limitations in the model have been discussed and the influence of coherent effects briefly assessed. Predictions show qualitative agreement with experimental observations. However, further developments of calculations and detailed comparisons with self-consistent simulations are required to facilitate a more quantitatively predictive model.

REFERENCES

[1] R. Baartman, "Betatron Resonances with Space Charge", in *Proc. Workshop on Space Charge Physics in High Intensity Hadron Rings*, Shelter Island, NY, 1998 *AIP Conf. Proc.*, CP448, pp.56–71.

[2] C. Warsop *et al.*, "Studies of Loss Mechanisms Associated with the Half Integer Limit on the ISIS Ring", in *Proc. HB2014*, East-Lansing, MI, USA, November 2014, paper MOPAB40, pp. 123–127.

[3] C. Warsop *et al.*, "Simulation and Measurement of Half Integer Resonance in Coasting Beams in the ISIS Ring", in *Proc. HB2012*, Beijing, China, November 2012, paper WEO1C02, pp. 434–438.

[4] M. Venturini *et al.*, "Resonance analysis for a space charge dominated beam in a circular lattice", *Phys. Rev. ST Accel. Beams*, vol. 3, p. 034203, Mar. 2000.